Solar Energy 205 (2020) 74–78

Contents lists available at ScienceDirect

Solar Energy

journal homepage: www.elsevier.com/locate/solener

Treatment of cyanide: Photoelectrocatalytic degradation using TiO_2 thin film electrodes and influence of volatilization

A. Brüger[a,*], G. Fafilek[a], M. Neumann-Spallart[b]

[a] Institute of Chemical Technologies and Analytics, Faculty of Technical Chemistry, Vienna University of Technology, Getreidemarkt 9, 1060 Wien, Austria
[b] Department of Inorganic Technology, University of Chemistry and Technology, Technická 5, 166 28 Prague 6, Czech Republic

ARTICLE INFO

Keywords:
Photoelectrocatalysis
TiO_2
Cyanide
Volatilization
Gold mining

ABSTRACT

Detoxification of waste water from gold processing is under increasing discussion in recent times. Limits for the release of cyanide are set to protect waterbodies and the soil surrounding gold processing facilities from contaminations.

Standards and limits are often based on varying data of the hazardousness. Notably concerning the volatilization of hydrogen cyanide and further reactions of HCN in the environment a variety of findings are published, with data, wide apart from each other, which influence the assessment of the hazard particularly for the workers in processing facilities. Likewise, the determination of the proper amount of volatilized cyanide in degradation experiments is essential for the accurate identification of the degraded part. In photoelectrocatalytic experiments, using TiO_2 films, light, and moderate electrical bias, the volatilization and the degradation rate of cyanide were determined at different pH. It is shown that the volatilization rate at pH $<$ 9 is predominant and cannot be neglected up to pH 13. Indirect vs. direct hole transfer on the semiconductor are discussed. With a new approach to the discussion of the comparability for different photocatalysts and varying experimental conditions we indicate a relationship between the rate constant of the degradation reaction and the difference of the energy of the valence band of the photocatalyst to the redox potential of oxidizable species.

1. Introduction

In cyanide leaching, the predominantly utilized process in gold extraction, the barren solution after the processing has to be treated for the reduction of the cyanide concentration. Exposure limits have been determined for the safety of the workers as well as the protection of the environment. In Table 1 some exposure limits of cyanide in air, water and soil, following EU directives and recommendations are listed, as well as the standards in China – the world's largest gold producer (USGS, 2018). These data are compared to the limits set in the international cyanide code, a voluntary initiative for the gold mining industries in this table.

The International Cyanide Management Code was developed as a consequence of the tailings spill at Baia Mare in Romania in 2000. Its intention is to secure a safe management with cyanide in reducing the exposure of workers and setting limits for the release of cyanide to the environment (ICMI, 2018). The cyanide code is widely implemented in gold mining and the number of signatory companies is still increasing. This initiative has made a contribution to reduce the risks in working with cyanide in the mining sector; however, the critical exposure values had to be adapted to the best practice in cyanide management. The high exposure limits of hydrogen cyanide in air, stated in the cyanide code - compared to the other data in Table 1 - are based on occupational exposure limits in leading gold mining countries but had to be modified to make sense in the context of the industry (ICMI, 2016). Even some of the lower limits for the exposure to air are based on research on the cyanide metabolization in human body that can hardly meet recent toxicological estimations (Loevenhart et al., 1918; Schulz et al., 1982; Brüger et al., 2018). Using established data where a level of 120 mg/m^3 over 1 h in humans may lead to death (WHO, 2004), with an average pulmonary cyanide absorption of 58%, a normal breathing respiratory minute volume of 7 L and a human body weight of 60 kg this would correlate to 8 µg/kg/min., compared to 17 µg/kg/min. from Loevenhart and 1 µg/kg/min. from Schulz. While these two values for metabolization in human body are still found in the literature (e.g. SCOEL, 2010; USEPA, 2010), Schulz et al. (1982) referred to fatalities at values of 2–3 µg/kg/min. Following these calculations, it seems advisable to limit cyanide exposure in air to less than 10 ppm, provided that it is compatible with best practice for management of cyanide.

A big part of the used cyanide in gold mines is released to the

* Corresponding author.
E-mail address: brueger@tuwien.ac.at (A. Brüger).

https://doi.org/10.1016/j.solener.2020.05.035
Received 30 January 2019; Accepted 14 May 2020

Table 1
Cyanide exposure limits in the EU, in China and listed in the international cyanide code (ICMC). STEL: short-term exposure limit (time – weighted average maximum airborne concentration over a 15 min. period), TSF: tailings storage facility, TWA: maximum average airborne concentration over an eight - hour working day, for a five - day working week, WAD: weak acid dissociable, MAC: Maximum Admissible Concentration, ceiling limit: maximum allowable human exposure limit. [1] EU (2017), [2] EU (2006), [3] EU (1998), [4] MOH (2007), [5] MEP (2007), [6] MOH (2006), [7] MEP (1996), [8] ICMI (2018).

	Exposure limit air	Tailings waste	Drinking water	Discharge to surface water	In stream limit (fresh water)
EU	STEL: 4.5 ppm cyanide TWA: 0.9 ppm cyanide [1]	56 mg/l WAD cyanide at the point of discharge into TSF as from 2008 and 11 mg/l as from 2018 [2]	0.05 mg/l total cyanide [3]		
China	1 ppm cyanide MAC [4]	0.8 mg/kg total cyanide solid waste [5]	0.05 mg/l cyanide [6]	0.5 mg/L total cyanide [7]	
ICMC [8]	10 ppm cyanide ceiling limit, 4.7 ppm in 8 h	50 mg/l WAD cyanide		0.5 mg/l WAD	22 µg/l free cyanide

atmosphere. An estimate of 30–50% given by NICNAS (2010) can hardly be correlated with current data of cyanide consumption in gold processing compared to gold production. A mass balance over the complete cyanidation process could help to identify potential high-risk areas. A crucial point for the risk assessment in gold processing facilities is the claim that hydrogen cyanide is oxidized in air and photolyzed by the sunlight, after volatilization, often referred to as natural degradation (TRI, 1998; MCA, 2005). Due to the fact that hydrogen cyanide is destroyed by UVC irradiation and the half-life is specified as 5 months to five years this should be neglected in the evaluation of danger areas surrounding gold processing facilities. Investigations in our laboratory have confirmed these findings (Brüger et al., 2018). Hence the process optimization for the reduction of cyanide volatilization in any section of gold processing considering the hazard potential as stated above would be an important contribution to minimize the HCN exposure of workers.

The reduction of remaining cyanide in gold processing via photocatalytic degradation is deemed to be a promising alternative to the established treatment processes. The most studied photocatalyst TiO_2 is either used as powder due to its simple application or in films supported on substrates with the advantages of reuse without catalyst separation and the optimized irradiation geometry of a catalyst film compared to a powder. With the coating of the catalyst on transparent conducting glass and applying of a moderate electrical bias, reduction of charge carrier recombination can be achieved, resulting in an increase of the degradation rate via photoelectrocatalytic processing.

In photocatalytic investigations of cyanide degradation, a varying outcome can be noticed as to degradation rates and degradation products as well. The degradation process of cyanide in general seems to depend mainly on the nature and amount of the oxidant and the pH. Besides the oxidation to cyanate, hydrolysis of cyanide and cyanate is discussed with NO_3^- besides NH_3/NH_4^+ and N_2 as products (e.g. Bravo et al. 1994, Augugliaro et al. 1997). In evaluating the possible products of the cyanide decomposition, the lack of an exact determination of the volatilized amount of cyanide should be considered. In former experiments in our laboratory, volatilization occurred in all process solutions with pH lower than pH 14. The loss of cyanide as HCN at high pH is established in the literature (Dhamo, 1996; Johnson, 2015). Disregarding the volatilization of HCN in photocatalytic as well as photochemical degradation experiments leads to results with higher degradation rates or the assumption of different secondary products. The cyanide loss in decontamination experiments in air is mainly attributed to natural oxidation and photolysis if the HCN volatilization is neglected (Li et al., 2005; Pérez et al., 2017; Shirzad Siboni et al., 2011).

Two further points should be addressed in experiments including air purging. As a consequence of the CO_2 content in air a decrease of pH is observed (in our experiments a drop from pH 13 to pH 12 in 48 h with an air flow rate of 12 L/h without bubbling through the solution) resulting in an increase of the cyanide volatilization rate in the course of the experiments. Simultaneously water from the solution is evaporated (in our experiments 8% in 48 h under the same conditions described above – 23.5 °C laboratory air, air conditioned, rH of 61%) resulting in an increase of the cyanide concentration at higher pH.

In this work we describe an approach that takes these factors into account for the exact determination of degradation values from the photoelectrocatalytic treatment of cyanide using a TiO_2 parallel plate flow-through reactor with a TiO_2 electrode. Furthermore, an attempt is made to compare our results with data of already published degradation experiments using different contaminants.

2. Experimental

2.1. Reactor setup

Photoelectrocatalytic reactions were studied using a parallel flow through reactor with back-side illumination (through the transparent support of the thin film catalyst layer). The solution was passed through a jacketed reaction flask in recirculating batch mode using a peristaltic pump with a flow rate of 45 L/h and kept at 23.5 °C (Fig. 1).

The volatilized hydrogen cyanide of the reaction solution was collected in an absorption flask via suction of air with a flow rate of 25 L/h. The air was passed through an absorption flask with glass diffuser prior to the reaction flask for the removal of CO_2 from the laboratory air and for humidification to prevent water evaporation during the experiments. The CO_2-free and humidified air was further passed through the reaction flask headspace without bubbling.

The reaction solution was a buffered KCN solution with a cyanide concentration of 400 mg/L (15.37 mM CN^-). pH 7.5 to 10.5 buffers were made with standard preparation methods (Bates and Bower, 1956). Cyanide analysis was done by titration against $AgNO_3$, following standard methods (SMWW APHA, 2012), modified for the use in our experiments. A detailed description of the cyanide analysis and further information on CO_2 removal and humidification are described elsewhere (Brüger et al., 2018).

2.2. Electrode properties.

The TiO_2 (anatase) electrode used in this study was prepared by spray pyrolysis at 470 °C on conducting glass plates (100 mm × 100 mm × 2 mm, spray deposited fluorine doped tin oxide on Duran glass, FTO with a sheet resistivity of 10–20 Ω). The thickness of the TiO_2 electrode was 400 nm, preparation and characterization have been described elsewhere (Shinde et al., 2008).

2.3. Photoelectrochemical setup

Photoelectrocatalytic experiments were carried out with a Solartron 1285 potentiostat over a period of 4 h. In the flow-through cell the TiO_2/FTO served as working electrode and electrical bias was applied against a polished stainless-steel counter electrode at a distance of 1.2 mm to the working electrode. The thin film reactor had a volume of

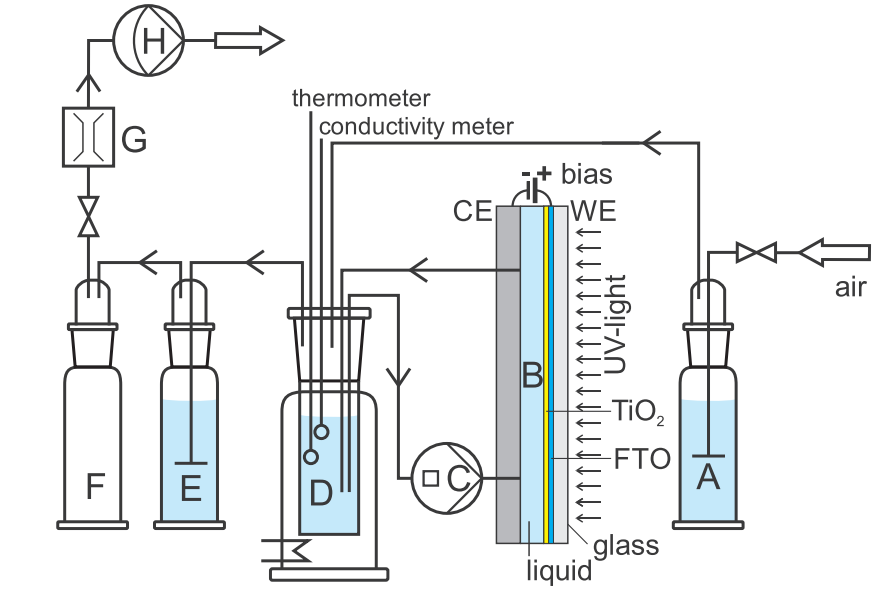

A. Absorption flask with fritted glass diffuser for CO_2 removal and H_2O saturation, pH 14
B. Thinfilm-reactor with UV-irradiation and external bias
C. Peristaltic pump
D. Reservoir (surface area: 16 cm^2) with sample solution, air circulation and temperature control
E. Absorption flask with fritted glass diffuser for absorption of volatilised HCN, pH 14
F. Suction flask trap
G. Rotameter
H. Vacuum pump

Fig. 1. Set-up for the photoelectrocatalytic experiments including the cyanide volatilization/absorption unit.

7 ml. The supporting electrolytes were the different buffers used for a constant pH consisting of KH_2PO_4, NaOH, HCl and $Na_2B_4O_7$. With an applied bias of 1.5 V vs. steel a photocurrent density of typically 0.4 mA/cm^2 was measured (illuminated area: 63 cm^2).

Irradiation of the photocatalyst was done from the backside through the transparent conducting substrate. UVA irradiation was provided by three fluorescent tubes (Sylvania Lynx BL350, 3x9W) with a wavelength maximum at 350 nm and a light irradiance of 66 W/m^2 between 320 and 390 nm at a distance of 4 cm. In Fig. 2 the spectrum of three Sylvania UVA lamps is illustrated with the absorption of Duran glass and the solar spectrum (direct + circumsolar light AM1.5, ASTM G-173).

Relative intensities of light emitted by the tubes as a function of wavelength were measured with an Ocean Optics fibre optic spectrometer. The radiation loss through the glass of the flask is approximately 15% in the used wavelength range as can be seen in Fig. 2. In fact, solar light contains photons in the UVA region which can be absorbed by TiO_2 and used in photoelectrochemical cyanide degradation.

3. Results and discussion

For the determination of the applied-bias range, where the current-potential curve is in a plateau region for the charge carrier separation, curves were generated in the dark and under illumination for every photoelectrocatalytic experiment. A typical i-E response curve under chopped light is illustrated in Fig. 3.

In the region of 1.5 V applied bias, a plateau is reached. Due to the fact that our reactor is for practical use, having a small (1.2 mm) gap between the electrode plates, there is no reference electrode in this system and thus no true potentiostatic control of the working electrode potential. The current potential curves reflect the ohmic drop of

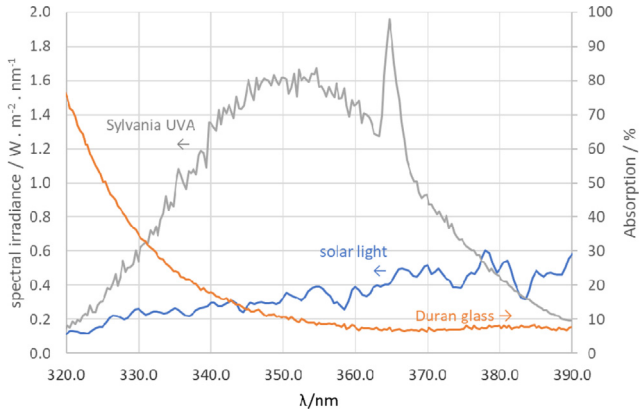

Fig. 2. Spectrum of UVA lamps, the absorption of Duran glass (thickness: 2 mm) and the solar spectrum (AM 1.5).

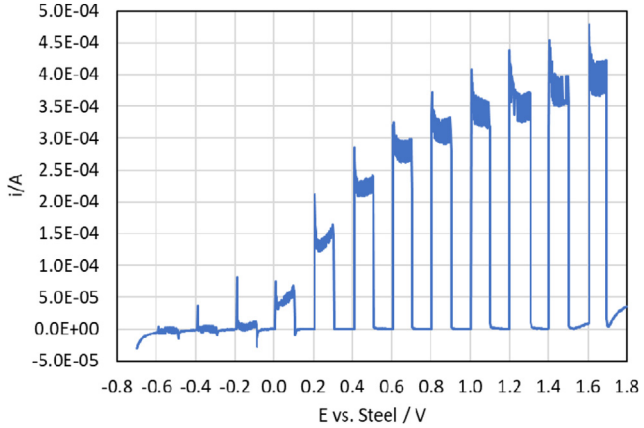

Fig. 3. Photoelectrochemical response of a TiO_2/FTO electrode in buffered solution pH 10, under slow rectangular chopped UVA light.

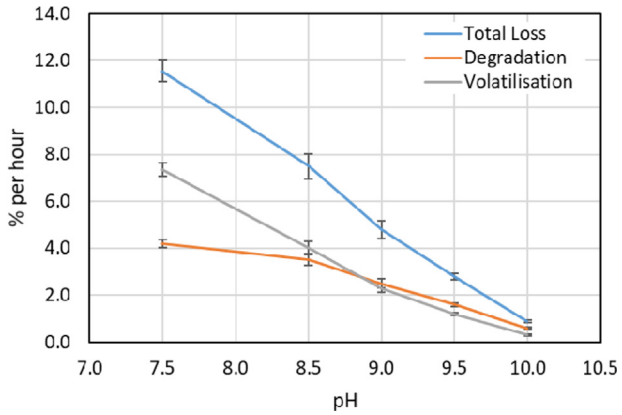

Fig. 4. Total and detailed cyanide loss in a degradation experiment, using 400 mg/l cyanide solutions in buffered solutions of different pH values. Initial loss values, in percent per hour.

electrolyte and working electrode as well as the polarization resistance of working and counter electrode. The aim of recording the photoelectrochemical response curve was to select an optimal value for the applied bias, where dark currents have not yet started rising and the charge carrier separation has already approached a maximum.

The photoelectrocatalytic degradation experiments using a moderate bias of 1.5 V, including the measurement of the volatilization of HCN are shown in Fig. 4.

In previous volatilization experiments without photoelectrocatalytic treatment, cyanate and hydrolysis due to oxygen in air and UV-irradiation was not observed (Brüger et al., 2018). Both, the degradation of CN^- and the volatilization of HCN decrease with increasing pH. For the determination of the volatilization behaviour of HCN, the HCN half-life in solution against the pH was determined in previous experiments (Brüger et al., 2018). The volatilization values are lower, compared to the degradation at high pH and higher below pH 9. As in the current investigations, the products were not analysed in detail, further analysis could bring knowledge about a possible influence of the different products.

Besides the increase of volatilization, the increase of cyanide oxidation with decreasing pH was confirmed. This would favour the hypothesis of a direct hole transfer mechanism (Eq. (2)) after the photogeneration of charger carrier pairs on the electrode (Eq. (1)):

$$\mathbf{TiO_2 + h\nu \rightarrow e^- + h^+} \tag{1}$$

$$\mathbf{CN^- + h^+ \rightarrow CN^{\cdot}} \tag{2}$$

where h^+ is a valence band hole, as reaction (2) does not involve hydroxide ions, whereas the valence band edge position changes with pH:

$$\mathbf{E_{vb} = E_{vb,pH=0} - 0.059pH} \tag{3}$$

The indirect route (Eqs. (4) and (5)) via trapping of photogenerated valence band holes by hydroxide ions (Wq. (4))

$$\mathbf{OH^- + h^+ \rightarrow OH^{\cdot}} \tag{4}$$

$$\mathbf{CN^- + OH^{\cdot} \rightarrow CN^{\cdot} + OH^-} \tag{5}$$

is independent of pH. Therefore, the observed pH dependence indicates that the direct route is prevailing. A more detailed investigation of the degradation behaviour of cyanide at lower pH should give appropriate information about this important aspect.

To make the experimental data comparable to investigations under various conditions as well as other photocatalysts, the rate constant (Eq. (6)) was normalized to the total volume (V) and to the photocurrent, i_{photo}, produced by photogenerated (UV light) charge carriers (Eq. (7)):

$$k = \frac{ln\frac{c}{c_0}}{t} \tag{6}$$

$$p = \frac{kVF}{i_{photo}} \tag{7}$$

c is the time dependent concentration of the solute being oxidized and p is a measure for the competition between oxidation of the added solute and oxidation of the solvent (water), Eq. (8), and reflects the interaction of the photocatalyst (surface properties) and the solute; F is Faraday's constant.

$$\mathbf{OH^- + h^+ \rightarrow \frac{1}{2}H_2O + \frac{1}{4}O_2 E_{O_2} = 0.4 + 0.059pOH} \tag{8}$$

In previous experiments, the authors have investigated the photoelectrochemical degradation of various organic compounds using TiO_2 (Shinde et al., 2009). In that study it was also shown that substantial photocurrents can be drawn from sunlight (174 μA/cm^2) Treatment of cyanide in the here reported experiments resulted in a low degradation rate compared to those investigations. This is due to the high redox potential of the cyanide radical, resulting in unfavorable competition with water oxidation (low p). In plotting p as obtained from this work and values of p calculated from published data (mainly of degradation of simple inorganic molecules), against the distance of the redox potential, E, of the species to be oxidized, to the potential of the valence band of the semiconductor (Eq. (3)), a correlation can be found which is visualized in Fig. 5.

For the plot of Fig. 5 data for photocatalytic degradation reactions using TiO_2 (rutile and anatase) and WO_3, another stable n-type photocatalyst, were assembled in order to show the applicability of this approach to different systems. The rate constant values in Fig. 5 increase with increasing difference between the redox potential of the valence band and the redox potential of the oxidizable species. This shows that, up to a certain extent, the thermodynamic driving force is the main factor governing the solute oxidation rate. The nature of the catalyst is of minor importance. The data however show a relatively wide scatter owing to the different methods used in the publications involved (see caption of Fig. 5). For an improved calculation, the degradation experiments should be carried out at different solution concentrations, which was rarely done. A second factor that could influence the degradation rate is the adsorption of the substances on the catalyst surface. Further investigation will have to be done to get more accurate data for the standardized rate constant relationship and to determine the influence of adsorption on the degradation rate. However, from the current data, the relationship becomes apparent and gives impetus for a deeper insight. The reason for the low oxidation rate

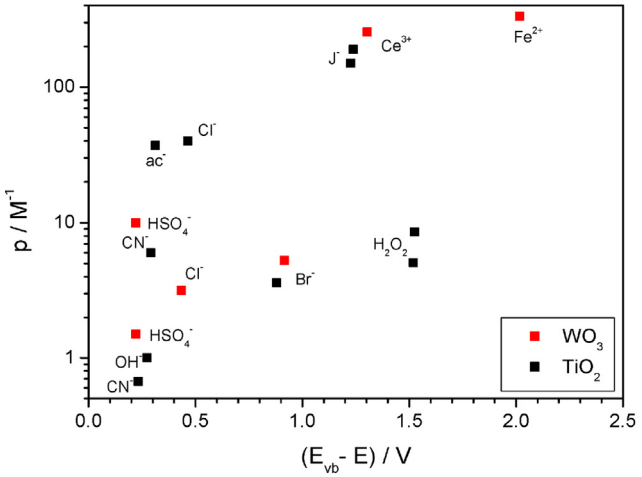

Fig. 5. Standardized rate constant – energy relationship. Constant p against the difference of the energy of the valence band to the redox potential of different species, using WO_3 and TiO_2 photocatalysts (data from Desilvestro and Graetzel, 1987; Frank and Bard, 1977; Hirano and Bard, 1980; Rappich and Dohrmann, 1990; Shinde et al., 2009; Kerchove et al., 1985).

of cyanide is clearly shown to be the high redox potential of this species.

4. Conclusions

For the determination of accurate data in degradation experiments of cyanide, a volatilization measurement equipment has to be integrated into the set up. Volatilization rates exceeded degradation in our experiments at lower pH. As the volatilized HCN is not destroyed by photolysis or oxidation in the surrounding atmosphere of the process, it represents a potential hazard in processing facilities, using cyanide.

The photoelectrocatalytic degradation efficiency of cyanide increases with decreasing pH. Only at high pH photoelectrocatalysis competes successfully volatilization of HCN. Cyanide-oxidation experiments will yield incorrect results if the determination of hydrogen cyanide volatilization is not included. The dependency of the photoelectrochemical cyanide ion oxidation on pH indicates the direct route of oxidation by valence band holes. The low degradation rate of cyanide using a TiO_2 photocatalyst compared to degradation reactions of other species on TiO_2 becomes apparent from a relationship of standardized rate constants and the difference of the valence band energy to the redox potential of the transfer of a single hole to the compound to be degraded. It could be shown that substances with a redox potential having a higher distance to the energy of the valance band, show a greater incentive to react on the catalyst surface. With the standardized rate constant relationship, the degradation behavior of different substances as well as various photocatalysts can be predicted and compared provided that the required data are available

Based on the current investigations, the analysis of degradation products at different concentrations and different pH as well as the adsorption properties will provide accurate conditions to optimize the photoelectrocatalytic degradation of cyanide, also with respect to degradation by sunlight.

References

Augugliaro, V., Loddo, V., Marci, G., Palmisano, L., Lopez-Munoz, M.J., 1997. Photocatalytic oxidation of cyanides in aqueous titanium dioxide suspensions. J. Catal. 166 (2), 272–283.

Bates, R.G., Bower, V.E., 1956. Alkaline solutions for pH control. Anal. Chem. 28, 1322–1324.

Bravo, A., Garcia, J., Domenech, X., Peral, J., 1994. Some observations about the photocatalytic oxidation of cyanate to nitrate over TiO2. Electrochim. Acta 39, 2461–2463.

Brüger, A., Fafilek, G., Restrepo, B.O.J., Rojas-Mendoza, L., 2018. On the volatilisation and decomposition of cyanide contaminations from gold mining. Sci. Total Environ. 627, 1167–1173.

Desilvestro, J., Graetzel, M., 1987. Photoelectrochemistry of polycrystalline n-tungsten trioxide. Electrochemical characterization and photoassisted oxidation process. J. Electroanal. Chem. Interfacial Electrochem. 238, 129–150.

Dhamo, N., 1996. Electrochemical oxidation of cyanide in the hydrocyclone cell. Waste Manage. (Oxford) 16, 257–261.

EU, 1998. Council Directive 98/83/EC of 3 November 1998 on the quality of water intended for human consumption Council of the European Union.

EU, 2006. Directive 2006/21/EC of the European Parliament and of the Council of 15 March 2006 on the management of waste from extractive industries and amending Directive 2004/35/EC European Union.

EU, 2017. Commission Directive (EU) 2017/164 of 31 January 2017 establishing a fourth list of indicative occupational exposure limit values pursuant to Council Directive 98/24/EC, and amending Commission Directives 91/322/EEC, 2000/39/EC and 2009/161/EU European Commission.

Frank, S.N., Bard, A.J., 1977. Semiconductor electrodes. 12. Photoassisted oxidations and photoelectrosynthesis at polycrystalline titanium dioxide electrodes. J. Am. Chem. Soc. 99, 4667–4675.

Hirano, K., Bard, A.J., 1980. Semiconductor electrodes. XXVIII. Rotating ring-disk electrode studies of photooxidation of acetate and iodide at n-type titanium dioxide. J. Electrochem. Soc. 127, 1056–1059.

Kerchove, F.V., Praet, A., Gomes, W.P., 1985. Kinetic investigation on the mechanism of the photoelectrochemical oxidation of water and of competing hole processes at the TiO_2 (rutile) semiconductor electrode. J. Electrochem. Soc. 132, 2357–2362.

ICMI, 2016. Personal communication. International Cyanide Management Institute, Washington, USA.

ICMI, 2018. Implementation Guidance for the International Cyanide Management Code. International Cyanide Management Institute, Washington, USA.

Johnson, C.A., 2015. The fate of cyanide in leach wastes at gold mines: An environmental perspective. Appl. Geochem. 57, 194–205.

Li, S., Zheng, B., Zhu, J., Yu, X., Wang, B., Natural cyanide degradation and impact on Ili River drainage areas from a Goldmine in Xinjiang autonomous region, China. Environ. Geochem. Health 27, 11–18.

Loevenhart, A.S., Lorenz, W.F., Martin, H.G., Malone, J.Y., 1918. Stimulation of the respiration by sodium cyanide and its clinical application. Arch. Intern. Med. 21, 109–129.

MCA, 2005. Fact Sheet – cyanide and its use by the minerals industry. Minerals Council of Australia, Kingston, Australia.

MEP, 2007. Standard of soil quality assessment for exhibition sites (Chinese standard HJ 350–2007). Ministry of Environmental Protection of the People's Republic of China, Bejing.

MEP, 1996. Integrated waste water discharge standard (GB 8978–1996). Ministry of Environmental Protection of the People's Republic of China, Bejing.

MOH, 2006. Standards of drinking water quality (GB 5749–2006). Ministry of Health of the People's Republic of China, Bejing.

MOH, 2007. Occupational exposure limits for hazardous agents in the workplace; Part 1: Chemical hazardous agents (GBZ2.1-2007), Ministry of Health of the People's Republic of. Bejing, China.

NICNAS, 2010. Sodium Cyanide. Priority Existing Chemical/Assessment Report 31, National Industrial Chemicals Notification and Assessment Scheme, Sydney, Australia.

Pérez, T., López, R.L., Nava, J.L., Lázaro, I., Velasco, G., Cruz, R., Rodríguez, I., 2017. Electrochemical oxidation of cyanide on 3D Ti-RuO2 anode using a filter-press electrolyzer. Chemosphere 177, 1–6.

Rappich, J., Dohrmann, J.K., 1990. Competitive photoelectrochemical processes as studied by in situ photocalorimetry: competition between the photoanodic oxidation of a solute (chloride, bromide, hydrogen peroxide, sulfite) and that of water at some n-type titania electrodes. J. Phys. Chem. 94, 7735–7739.

Schulz, V., Gross, R., Pasch, T., Busse, J., Loeschcke, G., 1982. Cyanide toxicity of sodium nitroprusside in therapeutic use with and without sodium thiosulphate. Klin. Wochenschr. 60, 1393–1400.

SCOEL, 2010. Recommendation from the Scientific Committee on Occupational Exposure Limits for Cyanide (HCN, KCN, NaCN). European Commission - Employment, Social Affairs and Inclusion.

Shinde, P.S., Sadale, S.B., Patil, P.S., Bhosale, P.N., Brüger, A., Neumann-Spallart, M., Bhosale, C.H., 2008. Properties of spray deposited titanium dioxide thin films and their application in photoelectrocatalysis. Sol. Energy Mater. Sol. Cells 92, 283–290.

Shinde, P.S., Patil, P.S., Bhosale, P.N., Brüger, A., Nauer, G., Neumann-Spallart, M., Bhosale, C.H., 2009. UVA and solar light assisted photoelectrocatalytic degradation of AO7 dye in water using spray deposited TiO_2 thin films. J. Appl. Catal. B: Environ. 89, 288–294.

Shirzad Siboni, M., Samarghandi, M.R., Yang, J.K., Lee, S.M., 2011. Photocatalytic removal of cyanide with illuminated TiO_2. Water Sci. Technol. 64 (7), 1383–1387. https://doi.org/10.2166/wst.2011.738.

Apha, S.M.W.W., 2012. 4500-CN^- cyanide. In: Rice, E.W. (Ed.), Standard Methods for the Examination of Water and Wastewater. American Public Health Association, Washington, DC, USA.

TRI, 1998. TRI/Right-To-Know Communications Handbook - Chemical Fact Sheets/Cyanide. Toxics Release Inventory, Environmental Health Center - A Division of the National Safety Council, Washington DC, USA.

USEPA, 2010. IRIS (Integrated Risk Information System) Toxicological Review of Hydrogen Cyanide and Cyanide Salts (Final Report). U.S. Environmental Protection Agency, Washington, DC, USA, EPA/635/R-08/016F.

USGS, 2018. Mineral Commodity Summaries – Gold. Report of the United States Geological Survey, Reston, Virginia, USA.

WHO, 2004. Hydrogen Cyanide and Cyanides: Human Health Aspects. Concise International Chemical Assessment Document 61. World Health Organisation, Geneva, Switzerland.